



# PECULIARITIES OF THERMAL AND HYDRODYNAMIC PROCESSES OCCURRING IN TIG AND A-TIG WELDING OF STAINLESS STEEL

D.V. KOVALENKO, I.V. KRIVTSUN, V.F. DEMCHENKO and I.V. KOVALENKO  
E.O. Paton Electric Welding Institute, NASU, Kiev, Ukraine

Analysis of distribution of temperature over the surface of the weld pool in TIG and A-TIG welding of stainless steel using the stationary and moving arc was carried out on the basis of calculation and experimental data. It is shown that in TIG and A-TIG welding the distribution of temperature over the weld pool surface above the boiling point has a characteristic plateau, the size of which is commensurable with size of the anode spot of the arc, the maximal temperature and size of this plateau being somewhat smaller in A-TIG welding. Problems of mathematical description and modelling of the Marangoni convection developing in A-TIG welding by the thermal-capillary and concentration-capillary mechanisms are discussed. Two circulation flows may form in the weld pool, their interaction causing a flow of the melt directed deep into the weld pool.

**Keywords:** TIG and A-TIG welding, stainless steel, stationary and moving arc, weld pool surface temperature, capillary Marangoni convection, force factors, penetration, experiment, mathematical modelling

The authors in their previous studies [1, 2] considered the phenomenological model of existence and interaction of the TIG/A-TIG arc-weld pool system, as well as the probability of existence of the quasi-keyhole in A-TIG welding. Peculiarities of the effect on formation of the weld pool and weld by thermal, mass exchange, electromagnetic, hydro- and gas-dynamic processes occurring in the arc column and weld pool in A-TIG welding using the stationary and moving arc were studied on the basis of analysis of experimental data and theoretical estimates. A substantial, fundamental difference in formation of the welds made by TIG and A-TIG welding with the moving and stationary arc was shown. This difference consists in the fact that in welding with the moving arc the processes of melting and solidification of the weld metal occur simultaneously, whereas in spot welding they are separated in time. Formation of the A-TIG spot weld is characterised by the presence of a specific deep crater with reinforcement on the weld periphery, which results from subsequent shrinkage phenomena. A fundamentally different formation of flows of the arc column plasma about the weld pool surface, directed from the periphery to centre, may take place in A-TIG welding, compared to TIG welding, this causing transfer of the overheated metal to the pool bottom and formation of the narrow and deep welds.

Study [3] offered a conjugate mathematical model of thermal, electromagnetic and hydrodynamic processes occurring in a weldment in stationary (spot) TIG welding. As established by modelling, parameters that determine the thermal state and hydrodynamics of the weld pool in arc welding are sizes of the anode (diameter of the current channel at anode) and heat

spots of the arc,  $R_a$  and  $R_h$ , respectively. The cardinal difference in penetrating capacity of the TIG and A-TIG welding methods is caused by a different proportion between sizes of the current and heat spots. Comparative analysis of the effect by three different force factors (Lorentz force, Marangoni effect, and Archimedes force) on the hydrodynamics and thermal state of the weld pool was carried out on the basis of results of experimental and calculation studies of the kinetics of penetration in TIG and A-TIG welding. At a small size of the anode spot (less than 4 mm), the dominant factor that determines depth and shape of the weld spot was shown to be a centripetal component of the Lorentz force.

Analysis of our results, as well as results of the studies performed by other authors, required additional experimental and theoretical investigations.

The purpose of this study was to conduct comparative analysis of experimental and calculation data on distribution of temperature over the weld pool surface, and consider peculiarities of capillary convection in TIG and A-TIG welding of stainless steel by using the stationary and moving arc.

**Peculiarities of distribution of temperature over the weld pool surface.** The calculations made by using the mathematical model [3] indicate to the probability of increase in density of the heat flow that exists at certain sizes of the anode and heat spots of the stationary TIG arc in welding of stainless steel 304, while this increase may lead to extra overheating of the weld pool surface to a temperature above boiling point  $T_b$ . This results in growth of heat losses for evaporation and decrease in assimilation of heat by the weldment. The temperature profile in overheating of the weld pool surface (in transverse direction) to a temperature above the boiling point has a characteristic plateau at  $T > T_b$  (Figure 1).

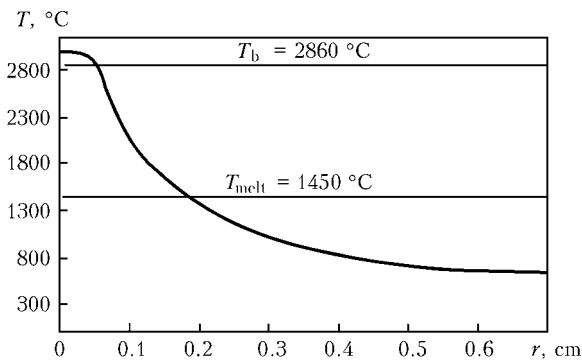


**Figure 1.** Calculated values of distribution of temperature over the weld pool surface in transverse direction at  $R_a = 1.25$  mm and  $R_h = 1.5$  mm;  $T_{\text{melt}}$  – melting temperature

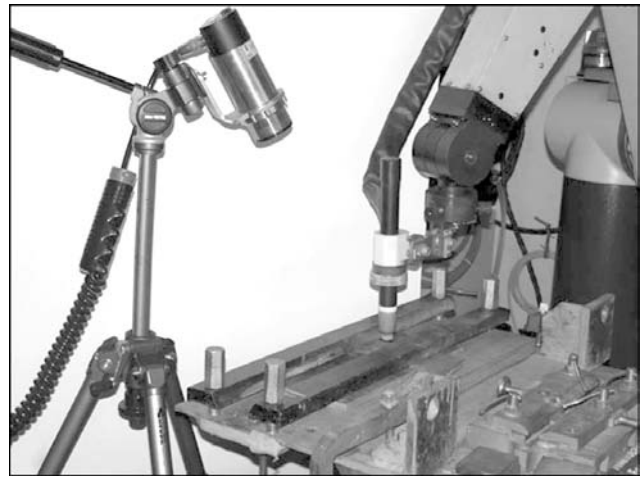


**Figure 2.** Appearance of experimental setup

An experiment on determination of the distribution of temperature over the surface of the weld pool along its axis was carried out to check the modelling calculation results. TIG and A-TIG welding with the moving arc was performed on a 5 mm thick specimen of stainless steel 304. Aerosol activating flux PATIG S-A was used for A-TIG welding. Welding conditions were similar to the calculated ones: welding current – 100 A, installed arc length – 1.5 mm, and welding speed – 100 mm/min. The tungsten electrode employed contained 2 %  $\text{ThO}_2$ , and had a diameter of 3.2 mm and sharpening angle of 35°. Argon was used as a shielding gas (flow rate – 12 l/min).

Appearance of the experimental setup is shown in Figure 2. «Raytek» computerised infrared pyrometer Marathon MM 1MH was used as a measuring device. Specifications of the pyrometer were as follows: range of temperatures measured – 650–3000 °C, spectral range – 1  $\mu\text{m}$ , error –  $\pm 0.3$  % or  $\pm 1$  °C, time of reaction – 1 ms, and measurement point diameter – 1 mm.

The fixed pyrometer was focused onto a point marked on the weld axis on the surface of a specimen welded. The weld pool formed by the arc moved through the marked point during welding. Simultaneously, the temperature on the surface of the weld pool was measured along its longitudinal axis. Schematic of the experiment is shown in Figure 3.

Results of the experimental studies are shown in Figure 4. In TIG and A-TIG welding with the moving arc the distribution of temperature over the weld pool surface above the boiling point has a characteristic plateau, the size of which is commensurable with that of the anode spot of the arc [4]. Diameter of this plateau for TIG and A-TIG welding is 1.75 and 1.5 mm, respectively. However, the maximal temperature of the plateau is somewhat lower in A-TIG welding (2600 °C), compared to TIG welding (2650 °C). Also, a somewhat increased level of temperature is observed in the tailing part of the weld pool in A-TIG welding.

It should be noted that the presence of this overheating plateau proved the probability of existence of the quasi-keyhole in A-TIG welding [1].

**Role of hydrodynamic processes and peculiarities of capillary convection in metal penetration.** One of the force factors affecting the hydrodynamics of the melt is Lorentz force, which is axisymmetric in the case of spot TIG and A-TIG welding, i.e.  $\vec{F} = \vec{F}(r, z)$ , where  $r$  and  $z$  are the radial and axial coordinates. The calculation data obtained in study [3] indicate that at a certain proportion of sizes of the anode and heat spots of the arc, and at anode spot radius  $R_a < 4$  mm, which are characteristic of A-TIG welding, the dominant force factor that determines

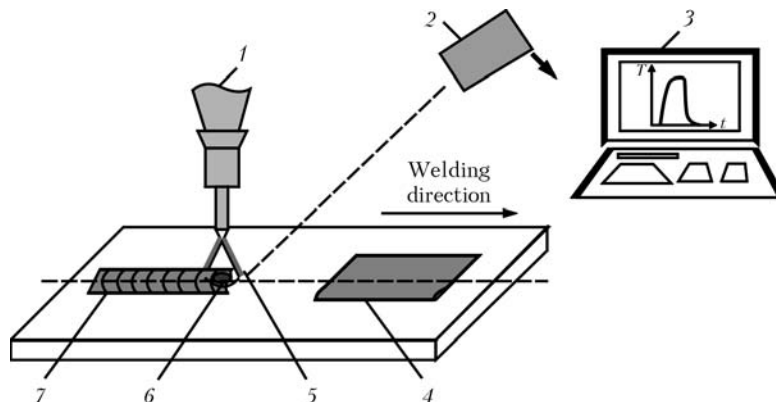


**Figure 3.** Schematic of experiment: 1 – torch; 2 – pyrometer; 3 – computer system with software; 4 – activator; 5 – arc; 6 – weld pool; 7 – weld

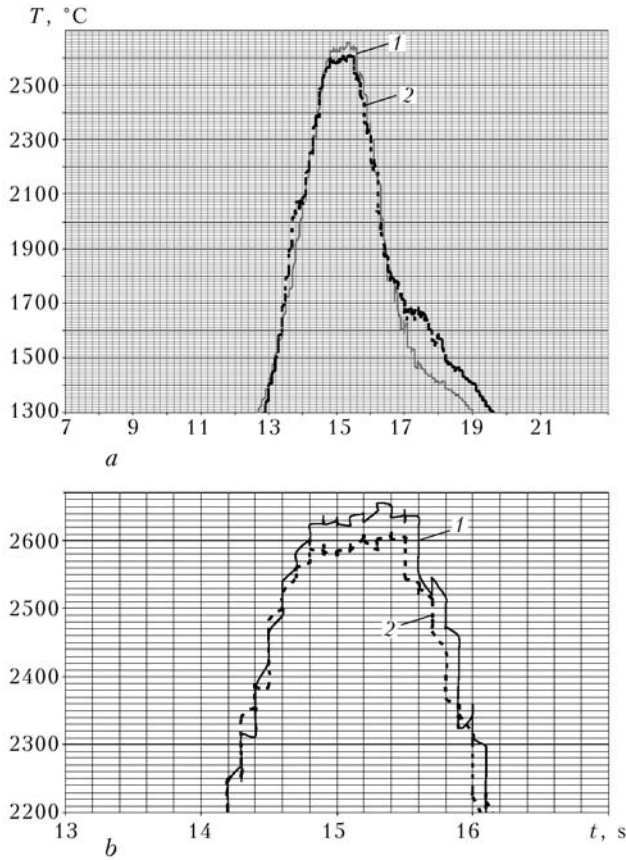


**Figure 4.** Experimental curves of distribution of temperature over the weld pool surface in longitudinal direction depending on welding time in temperature ranges of 1300–2800 (a) and 2200–2800 (b) °C: 1 – TIG welding; 2 – A-TIG welding

the hydrodynamics of the weld pool is a radial component of the Lorentz force, which is centripetal at the axisymmetric magnetic field. It should be noted that for the weld pool surface this force in the anode spot is directly proportional to squared welding current  $I^2$  and inversely proportional to cubic anode spot radius  $R_a^3$  [1, 2]:

$$\vec{F}_{rot}(r, 0) = -\mu_0 \frac{I^2}{4\pi R_a^3} \frac{r}{R_a} \vec{e}_r, \quad 0 < r < R_a,$$

where  $\mu_0$  is the relative magnetic permeability, and  $\vec{e}_r$  is the unit radius vector.

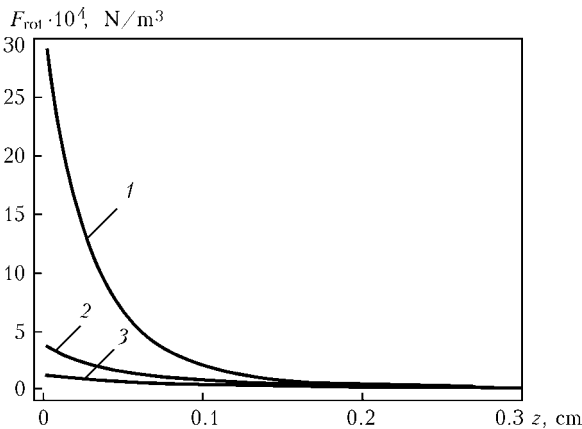


**Figure 5.** Calculated values of  $F_{rot}(R_a, z)$  along axial coordinate  $z$  at  $I = 100$  A: 1 –  $R_a = 1$ ; 2 – 2; 3 – 3 mm

The effect of the size of the anode spot on the centripetal component of the Lorentz force is shown in Figure 5.

The vortex flow of the melt forms in the weld pool under the effect of the centripetal component of this force. Near the free surface this flow is directed from the periphery toward the weld pool centre. The molten metal flows moving from the opposite directions turn in the axial part of the pool to the axial direction, transporting the metal overheated to the boiling point or higher (see Figures 1 and 4) from the centre of the heat spot toward the pool bottom. As the speeds of movement of the molten metal are kept at a sufficiently high level (max  $|\vec{V}| \approx 50$  cm/s), the moving melt retains much of overheat, thus leading to densification of temperature with a high temperature gradient in the weld pool near the melting front. This creates conditions for increase in the penetration depth.

Consider the effect of capillary convection (Marangoni effect) on penetrating power of the arc in A-TIG welding. It is a known fact that surface-active elements influence the surface tension coefficient of metal. Oxygen, sulphur, fluorine etc. may serve as surface-active elements that get from the flux to the melt in A-TIG welding. For example, as established in study [5], surface tension coefficient  $\gamma$  as a function of oxygen content  $C$  in steel grows with decrease in the oxygen concentration ( $\beta_C = \partial\gamma/\partial C < 0$ ). As the oxygen concentration on the weld pool surface decreases with increase in temperature,  $\partial C/\partial r > 0$  and, hence,  $\beta_C \partial C/\partial r < 0$ . This is indicative of the probability of formation of the reverse concentration-capillary Marangoni convection caused by the oxygen concentration gradient on the free surface of the weld pool.

At the same time, according to the data of study [6], temperature surface tension coefficient  $\beta_T = \partial\sigma/\partial T$  of the iron melt with an oxygen content of  $(150-350) \cdot 10^{-6}$  takes a positive value within a temperature range of 1873–2123 K. Hence,  $\beta_T \frac{\partial T}{\partial r} < 0$ , this being indicative of the probability of the direct thermal-capillary convection. If the concentration-capillary and thermal-capillary convections combine, the condition of balance of tangential stresses on the free surface of the melt can be written down as

$$v \frac{\partial V_r}{\partial z} \Big|_{z=0} = -\frac{1}{\rho} \left[ \beta_T \frac{\partial T}{\partial r} + \beta_C \frac{\partial C}{\partial r} \right].$$

Therefore, A-TIG welding features the probability in principle of formation of the reverse (from the periphery of the pool toward its centre) Marangoni flow caused by both thermal-capillary and concentration-capillary mechanisms. To experimentally determine  $\beta_T$  and  $\beta_C$ , it is extremely important to provide the necessary conditions for finding partial derivatives



$\partial\sigma/\partial C$  and  $\partial\sigma/\partial T$ . Otherwise the experimental data may be noisy.

High-temperature heating of metal up to the boiling point,  $T = T_b$ , takes place in the central part of the weld pool surface in the overheating plateau region. As follows from physical considerations,  $\gamma(T, C) \rightarrow 0$  at  $T \rightarrow T_b$ , independently of the oxygen content. This means that

$$\partial\sigma/\partial r = \beta_T \frac{\partial T}{\partial r} + \beta_C \frac{\partial C}{\partial r} > 0$$

within a certain temperature range ( $T_{\text{ext}} < T < T_b$ , where  $T_{\text{ext}}$  is the extreme temperature) below the boiling point, i.e. the surface tension coefficient at certain definite temperature  $T = T_{\text{ext}}$  has a maximum, and direction of the surface force in this temperature range corresponds to the direct (from the centre to periphery of the pool) capillary convection. Therefore, the opposite, as well as direct (from the centre to periphery of the weld pool at  $T \in [T_{\text{ext}}, T_b)$  and reverse (from the periphery of the weld pool to its centre at  $T < T_{\text{ext}}$ ) capillary convections may simultaneously exist on the weld pool surface in A-TIG welding. In this case, two vortexes may form in the weld pool, the interaction of which results in the flow of the melt directed deep into the weld pool.

It should be noted in conclusion that, in our opinion, the available experimental data on dependencies

$\beta_C = \beta_C(T, C)$  and  $\beta_T = \beta_T(T, C)$  within a wide temperature range are insufficient to theoretically estimate with certainty the effect by the Marangoni convection on the penetrating capacity of A-TIG welding. Investigation of this effect requires additional experimental studies of the dependence of the surface tension coefficient on the temperature and concentration of an activating element in the melt, especially for the conditions of interaction of the flux layer with the weld pool surface.

1. Paton, B.E., Yushchenko, K.A., Kovalenko, D.V. et al. (2006) Role of quasi-keyhole and Marangoni convection in formation of deep penetration in A-TIG welding of stainless steel (Phenomenological model of A-TIG welding of stainless steel). In: *Proc. of Joint 16th Int. Conf. on Computer Technology in Welding and Manufacturing and 3rd Int. Conf. on Mathematical Modelling and Information Technologies in Welding and Related Processes* (Kiev, Ukraine, June 2006). Kiev: PWI, 258–263.
2. Yushchenko, K.A., Kovalenko, D.V., Kovalenko, I.V. et al. (2007) Phenomenological model of existence and interaction of the system of activated arc and liquid channel of metal pool in A-TIG welding. *IW Doc. XII-212-1112-07*.
3. Yushchenko, K.A., Kovalenko, D.V., Krivtsun, I.V. et al. (2008) Experimental studies and mathematical modelling of penetration in TIG and A-TIG stationary arc welding of stainless steel. *IW Doc. XII-212-1117-08*.
4. Yushchenko, K.A., Kovalenko, D.V., Kovalenko, I.V. (2003) Investigation of peculiarities of A-TIG welding of stainless steels. *IW Doc. 212-1047-03*.
5. Lancaster, J.F., Mills, K.C. (1991) Recommendations for the avoidance of variable penetration in gas tungsten arc welding. *IW Doc. 212-796-91*.
6. Taimatsu, M., Nogi, K., Ogino, K.J. (1992) Surface tension of liquid Fe-O alloy. *High Temp., Soc. Jap.*, 18(1), 14–19.

## RISK OF FORMATION OF CARBIDES AND $\alpha$ -PHASE IN WELDING OF HIGH-ALLOY CHROME-NICKEL STEELS

V.I. MAKHNENKO<sup>1</sup>, S.S. KOZLITINA<sup>1</sup>, L.I. DZYUBAK<sup>1</sup> and V.P. KRAVETS<sup>2</sup>

<sup>1</sup>E.O. Paton Electric Welding Institute, NASU, Kiev, Ukraine

<sup>2</sup>Rivnenskaya NPP, Kuznetsovsk, Ukraine

The possibility is considered of using calculation methods to predict the risk of formation of the  $\sigma$ -phase in the HAZ metal of chrome-nickel steels at a carbon content of about 0.08 % and higher. It is shown that the use of temperature-time constitutional diagrams for steel of a corresponding composition, combined with temperature cycles at points in the HAZ metal, allows predicting the degree of sensitization of the corresponding HAZ region under different welding conditions.

**Keywords:** arc welding, chrome-nickel steels, welded joints, sensitization,  $\sigma$ -phase, intergranular cracks, stress corrosion, temperature-time diagram

Problem of formation of the third phases is one of the fundamental in welding of austenite chrome-nickel steels with increased content of carbon. Corresponding recommendations were developed for its solving and included in many reference books [1 and others]. It is characteristic that mentioned third phases (besides initial austenite and ferrite) appear after a primary crystallization during some soaking at specified temperature interval (Figure 1). They made no serious problems for the near-weld zone metal in a single run

welding. An overlay of the curves of thermal cycles for specific points of the near-weld zone on respective temperature-time diagrams (*c*-curves) for steel of a corresponding composition (Figure 2) in multi run welding, however, shows that the accumulation of conditions for formation of the chromium carbides along the grain boundaries (due to diffusion of carbon controlled by *c*-curve in Figure 2, *a*) or  $\sigma$ -phase accumulation due to  $\delta$ -ferrite decay and formation of complex intermetallics (Figure 2, *b*), also controlled by diffusion processes, occur in the near-weld zone. Avrami method [2, 3] with coefficients, determined depending on temperature and level of formation of